Synchronized Uplink Time of Arrival Localization: A Measurement-driven Evaluation

Keerthi Priya Dasala
Rice University
Houston, TX, USA
keerthi.dasala@rice.edu

William M. MacDonald
Bell Labs, NOKIA
Murray Hill, NJ, USA
mike.macdonald@nokia-bell-labs.com

Dragan Samardzija
Bell Labs, NOKIA
Crawford Hill, NJ, USA
dragan.samardzija@nokia-bell-labs.com

2020 IEEE 92nd Vehicular Technology Conference (VTC2020-Fall) | 978-1-7281-9484-4/20/$31.00 ©2020 IEEE | DOI: 10.1109/VTC2020-Fall49728.2020.9348632

***Abstract*—We study terrestrial wireless uplink Time of Arrival (ToA) localization systems where multiple infrastructure nodes measure the ToA from the signal transmitted by a user of interest. The measured ToA is shared with a centralized server that then computes the location of the device. While the fundamental issues such as accurate synchronization and accurate location of nodes concerning precise location estimation have been addressed elsewhere, we mainly focus on improving the efficiency of ToA estimation in this work. Using our proposed methodology, a 30 fold improvement in the computational efficiency at no cost of localization accuracy was observed which in practice enables the localization network to track and coordinate many more simultaneous users frequently. We validated our ToA estimates on the over-the-air measurements taken from our on-campus localization network and obtained sub-meter accuracy, indicating that our solution is competitive with conventional high overhead ToA methods.**

***Index Terms*—E911, LLS, Localization, Multipath, radio-based Positioning, Synchronization, ToA, UTDoA, White Rabbit, WLLS**

I. Introduction

In recent years, location based services have gained lot of importance as it plays a vital role in provisioning reliable long-range to short-range communication and can enable applications that depend on a user's location to provide services such as tracking, navigation, healthcare and billing. The core of these services is the positioning technologies which come in many different flavors and requirements in the sense that achieving centimeter level accuracy might be straightforward in some cases while achieving less than ten meters localization error seems unthinkable in other cases. For instance, we rely on Global navigation satellite systems (GNSS) such as GPS and GLONASS with real-time kinematic (RTK) positioning for centimeter accuracy localization outdoors and achieve centimeter accuracy using ultrawideband (UWB) systems [1] indoors. Both these systems employ (ToA) measurements for positioning objects. Unlike non-overlay systems like WiFi and LTE which serve the dual role of both communication and localization, these overlay systems are deployed for the sole purpose of localization.

In this paper, a non-overlay deterministic system that is based on ToA is discusses. However, achieving the desired level of localization accuracy depend on precise ToA measurements and in practice, this precision comes with a set of fundamental challenges. For example, in wireless channels with multipath fading, unresolvable multipath can result in a positive bias error in the ToA estimate. Recall that multipath components can be resolved if the delay between paths is greater than the reciprocal of the signal bandwidth. If the Line-Of-Sight (LOS) component is indistinguishable from an Non-Line-of-Sight (NLOS) multipath component, the maximum value of this peak is different compared to the LOS arrival time. This bias error depends on the relative amplitudes, timing difference and phase of the components and could be as large as the time difference between the paths. This problem can be resolved at the expense of higher bandwidth and high SNR.

The issue of multipath has been described extensively in [2] [3] but even in the absence of unresolvable multipath and in the presence of high SNR, bandwidth limits the temporal resolution of the ToA. One way to address this issue is to interpolate the received signal or the correlation of the received signal with the known transmit signal to improve the temporal resolution. In [4] this provided accurate ToA estimations and localization using a high overhead interpolation method.

Our work in effect provides a 30 fold improvement over the existing high overhead ToA methods by proposing a computationally efficient ToA estimation method. In particular, we build on the benefits of various low overhead interpolation methods for calculation of ToA estimate in order to improve the computational efficiency. These ToA estimates are then validated on the over-the-air measurements obtained from a real deployed on-campus localization network. We demonstrate that our computationally inexpensive solution achieves about $\leq 1\%$ degradation in localization error over the high overhead ToA method with $30\times$ improvement in processing time. This indicates that our solution would be at least, competitive with existing traditional methods to track and coordinate many simultaneous users frequently.

II. Time of Arrival Localization: Proposal

A. Primer on Time of Arrival Localization

Time of arrival localization can be broken down into system that use an uplink reference signal and those that use a downlink reference signal. In the uplink ToA approach, the device to be localized (rover) sends out a signal that is received by several nodes (sniffers). Each sniffer shares its ToA information with a centralized server that then computes

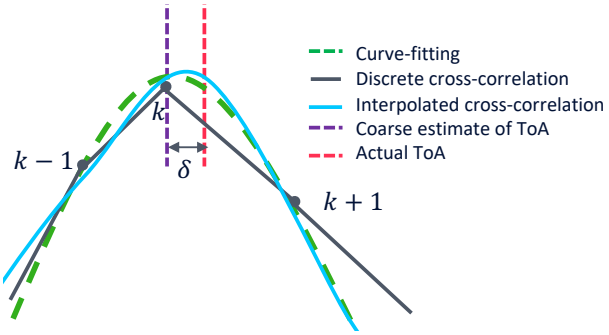

Fig. 1: An illustration of the curve fitting to the discrete cross correlation peak.

the location of the rover. In this case the desired information, the rover location, resides in the network.

The localization estimation starts with the pseudorange equation that has been covered extensively in the literature [5]. The system that will be described in this paper uses the uplink ToA approach and consists of a rover at unknown cartesian coordinates (x_r, y_r, z_r) and several sniffers at location (x_i, y_i, z_i) where i refers to the i^{th} sniffer. Solving for (x_r, y_r, z_r) requires a minimum of four pseudorange equations – one for each of the unknowns which also includes the clock offset between the rover and the sniffer. The main challenges in estimating the location of the rover using this method are accurate synchronization of the sniffers, accurate location of the sniffers, and an accurate determination of the ToA. While all three of these issues were addressed in a previous paper [4], the approach was computationally intensive and thus impractical.

B. Proposal

The received signal I/Q samples are recorded at the location server for post processing. The first step is to correlate the rx signal with a local replica of the tx signal. The periodic discrete cross correlation between the reference and received signals $x(k)$ and $y(k)$ with a period of N_p samples is

$$r_{xy}(n) = \sum_{k=1}^{N_p} x(k)y(k+n) \tag{1}$$

where n is the lag. Circular convolution can be performed more efficiently using the Fast Fourier Transform (FFT), especially for large N_p.

$$R_{xy}(n) = X(n)Y(n)^{\dagger} \tag{2}$$

where R_{xy}, X and Y are the discrete Fourier Transforms of r_{xy}, x and y, and $\dagger$ denotes the complex conjugate.

A more precise estimation of the first arrival time is found by interpolating the correlation signal in the neighbourhood of the first arriving peak.

Frequency domain interpolation: The interpolation is done in the frequency domain by inserting zeros in the out-of-band portion of the spectrum to achieve the desired level of interpolation and then an inverse FFT returns the upsampled time-domain correlation. The peak in the interpolated data is used as the arrival time and this peak is roughly located in the range of ± 1 sample about the first arriving peak in the uninterpolated correlation.

Three point Interpolation: The frequency domain interpolation is computationally expensive depending upon the required granularity of interpolation. For example, in order to achieve a localization accuracy of $< 10\ cm$, the time between the samples needs to be atleast 300 ps or better. In standard localization systems using LTE with a bandwidth support of 20 MHz and a time resolution of 32 ns, the frequency domain interpolation would require an interpolation factor above 100 to arrive at desired localization accuracy and this can be potentially prohibitive due to the large computation overhead. To workaround this problem, we simplify the estimation of the arrival time by interpolating only the immediate neighbors (two points $(k-1)$ and $(k+1)$ surrounding the peak (k) in the uninterpolated data as illustrated in Fig. 1. Hence this method is called as three point interpolation and the following methods have been used in our study.

Parabola: This method fits a parabola to three points [6] and the peak of this parabola can then be found, indicating a subsample estimate of the delay. If the peak of the cross correlation is at $r_{xy}(k)$, the interpolated peak is at a delay of

$$\hat{t}_d = k + \frac{r_{xy}(k-1) - r_{xy}(k+1)}{2(r_{xy}(k-1) - 2r_{xy}(k) + r_{xy}(k+1))} \tag{3}$$

Gaussian: A Gaussian curve could be fitted to the three points surrounding the cross correlation peak [7], using $\hat{r_{xy}}(t) = ae^{-b(t-c)^2}$ which has a peak at a delay of

$$\hat{t}_d = k + \frac{ln(r_{xy}(k-1) - r_{xy}(k+1))}{2(ln(r_{xy}(k-1)) - 2ln(r_{xy}(k)) + ln(r_{xy}(k+1)))} \tag{4}$$

and is equivalent to fitting a parabola to the logarithm of the data.

Cosine: A cosine could be fitted to the three points [8], [9], using $\hat{r_{xy}}(t) = acos(\omega t + \phi)$. The interpolated peak may be calculated using

$$\omega = acos\left(\frac{r_{xy}(k-1)+r_{xy}(k+1)}{2r_{xy}(k)}\right) \tag{5}$$

$$\phi = atan\left(\frac{r_{xy}(k-1)-r_{xy}(k+1)}{2r_{xy}(k)sin(\omega)}\right) \tag{6}$$

$$\hat{t}_d = k - \frac{\phi}{\omega} \tag{7}$$

Two point Interpolation: This method [10] first finds the peak of the cross correlation signal r^*_{xy} of zero mean normalized signals of x^* and y^*.

$$x^* = \frac{x - \bar{x}}{||x - \bar{x}||_2}, \quad y^* = \frac{y - \bar{y}}{||y - \bar{y}||_2} \tag{8}$$

where $\bar{x}$ denotes the mean and $||\cdot||_2$ denotes the Euclidean norm. This peak and the larger of its two neighboring values are assumed to bracket the subsample peak on the interval between delays $k-1$ and k. If one assumes that the signals are linearly interpolated between samples, a nonlinear equation for the cross correlation between peaks can be found, which

has a maximum given by the analytical equation

$$\hat{t}_d = k + \frac{r^*_{xy}(k-1) - a r^*_{xy}(k+1)}{(a-1)(r^*_{xy}(k-1) + r^*_{xy}(k))} \quad (9)$$

where a is the autocorrelation of r^*_{xy} at a delay of one sample. **Note:** In practice, there may be a peak hopping or false peak errors, that is the time delay corresponding to the main peak maybe mistaken for the subsidiary peak due to the estimation variance of the correlation function. As a result, curve fitting via interpolation locally applied around the peak, can have guaranteed improvement in estimation accuracy only in cases of zero peak ambiguity.

III. Localization Network

To explore the challenges presented in the previous section, a prototype system was constructed consisting of five sniffer nodes and a rover. The details of the system will be discussed in the next subsections.

A. Hardware Details

Each sniffer node and the rover used a Software Defined Radio (SDR) platform based on the National Instruments nanoBEE platform. This platform provides a bandwidth of 55MHz, an output power of +23 dBm, and four transmit and receive chains. The TX and RX sample rates were 61.44 MHz and each sample was 12 bits. The IQ samples for the transmitter and receiver originated and terminated, respectively, from a Xilinx Z-7100 FPGA. The transmit and receive samples were stored in Block RAM and sent to the transmit antenna as needed or stored in Block RAM on the receiver side. The Block RAM space limited capture to 32760 samples. Periodically, the receive samples were send back to the location server where the user location was determined offline.

An outdoor deployment was chosen that, from a GNSS perspective, closely imitated an urban environment. That is, the GNSS satellite reception was so poor that an RTK GNSS fix was only possible in a limited number of locations. Furthermore, the sites for the sniffers were chosen to provide both Line of Sight (LOS) and NLOS links to the rover. A picture of the deployment space and the location of the sniffers is shown in Fig. 2.

The sniffers are denoted by the red circles and the accompanying numbers, in the white ellipses, are used elsewhere in the text. The blue squares represent the fifteen measurement locations. Measurement location ten, in the square box, are discussed later in the text. The green dashed area encloses the expected location of the rover.

The antenna and rover location were determined using conventional surveying equipment know as a total station [11] which provided an accuracy of less than one centimeter relative to the ground truth established by RTK GNSS. The degree of synchronization among the sniffer nodes is critical to the success of ToA localization. The synchronization among the sniffer nodes was achieved by using White Rabbit protocol [12], [13] and this provded subnananosecond time

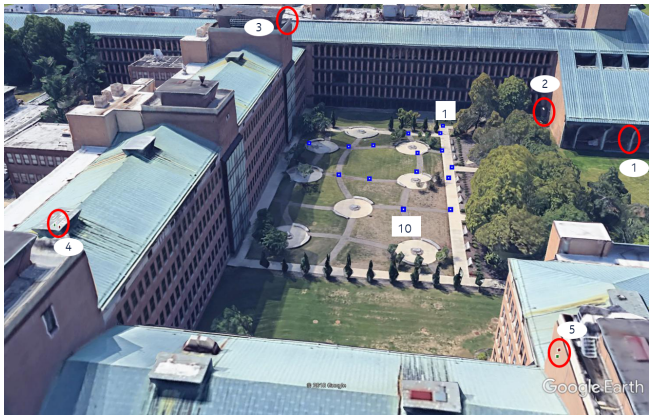

Fig. 2: Murray Hill Campus with measurement points(blue squares) and sniffer locations(red circles) indicated

synchronization across all five nodes and a jitter of less than 200 ps at each node.

B. Signal processing

The transmit waveform was a root raised cosine filtered maximal length sequence that was directly modulated onto the I and Q RF signals. This waveform was chosen for its excellent processing gain of 36 dB (high SNR), thus eliminating the need for a power amplifier at the rover. The signal was transmitted at a center frequency of 3.495 GHz with a bandwidth of 50 MHz from an omnidirectional antenna with 5 dBi gain. The transmission was initiated on a pulse per second that was supplied either from a GNSS receiver or from the White Rabbit IP core. At the sniffer, the signal was received by a dual polarization antenna with 16 dBi gain. Cables at the sniffers were all the same length and delays were measured and used as a correction for the ToA measurements. The sniffer data acquisition was triggered on the PPS from the White Rabbit IP core and continued until the block RAM was filled. The maximum data recorded at the sniffer was eight transmit sequences or 533 μs. The data are transmitted back to the location server and the measurement was repeated on the next PPS boundary. At the location server the signal processing sequence can be broken down into three distinct tasks. In the first task, the first arriving multipath component is determined from the correlation of the TX and RX signals, next the arrival time of this path is determined precisely by interpolating the correlation peak of the first path, and finally the LLS algorithm is performed to determine the x, y, and z coordinates from the arrival time measurements. The I and Q samples are recorded at the location server for post processing.

IV. Proof of Concept Experiments

Measurements were collected at fifteen locations in the measurement space shown in Fig. 2. For these measurements, the transmitter as well as the receivers were synchronized to White Rabbit ensuring that all nodes were synchronized to within one nanosecond. While White Rabbit can provide subnanosecond synchronization, additional uncontrolled

delays can occur through the FPGA and the transmit and receive chains so all sniffers were synchronized to less than one nanosecond. Even with these delays, the system was stable to 200 ps. Samples were collected for a period of five to fifteen minutes at each of the fifteen locations to get meaningful statistics on the time of arrival. While all samples were recorded on all twenty receive antennas at the five sniffer locations, only the vertical polarization data are presented in this paper.

A. Time of Arrival Estimation

As a first step, the correlation is carried out in the frequency domain and then an inverse Fourier transform is carried out to return to the time domain [14]. A typical output from the correlator is shown in Fig. 3a. Any peaks that come prior to the maximal peak are accepted provided they are no more than 10 dB below the maximal peak and are 7 dB above the noise floor. With this procedure, the green circle was determined to be the first arriving peak. The close agreement between the green circle and the green dotted line (the geometric time of flight) suggests that the correct peak was determined and that the measured internal delays are correct.

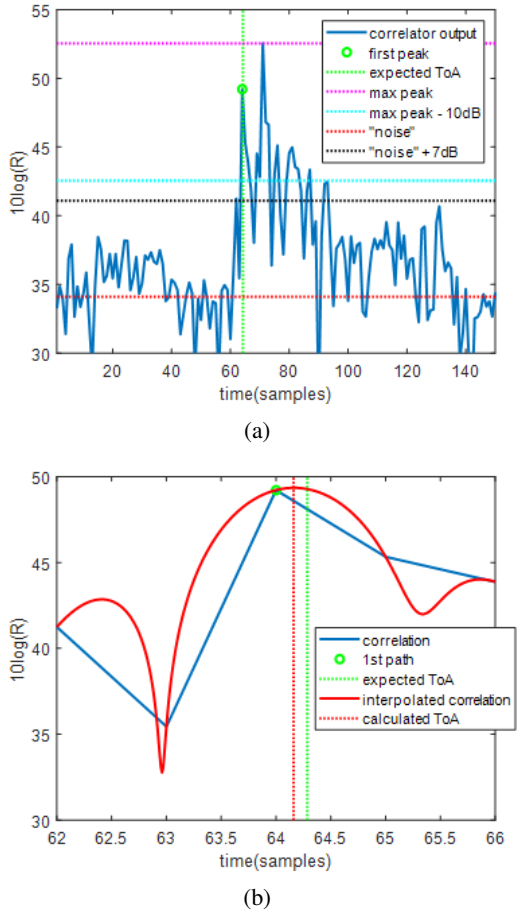

Fig. 3: a) Example of the correlator output from the collected measurements b) Interpolation of the correlator output.

Next, the subsample time delays were estimated using the methods described in Sec. II-B. The outcome of the frequency domain interpolation is shown in Fig. 3b. In this instance the interpolator underestimated the arrival time by approximately 2 ns. Such errors are present in most of the correlation peaks and are most likely a result of unresolvable multipath. A higher bandwidth system is required to verify this assertion.

B. Time of Arrival Bias

In a five minute interval approximately 900 sequences are recorded resulting in 900 estimations of the ToA, from each of the ten antennas in the network. The locations of the rover and sniffers are known from the survey and results in an accurate knowledge of the geometric distance from sniffer to rover and thus, the expected time of flight. Although the cable delays in the SDR and antennas were all calibrated, there can still be some uncertainty in the clock synchronization between the sniffers and the rover, which will result in localization estimation errors [15]. These errors can be compensated by measuring the ToA bias and subtracting it from the measured ToA. This calibration step can be done at one or multiple measurement points. In the lab these errors were less than one nanosecond. It is not possible to measure the synchronization error once the system is deployed. Such synchronization errors

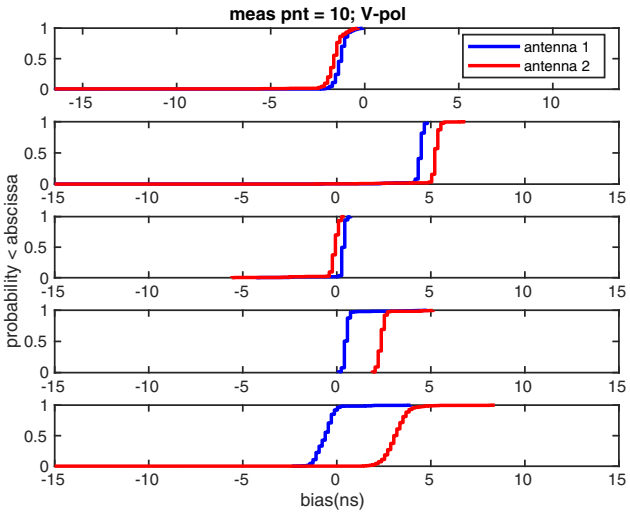

Fig. 4: Empirical CDF obtained by frequency domain interpolation at the five sniffer locations for the both vertically polarized antennas for measurement location 10. The subplots are for sniffers 1-5 from top to bottom

will result in localization estimation errrors [15] but can be removed by measuring the ToA bias that results from this synchronization errors and subtracting then from the measured ToA. This calibration step can be done at at one or multiple measurement points. The timing bias referred to as τ_{bias} is any delay that cannot be accounted for such as multipath delay and synchronization errors and is defined as follows

$$\tau_{bias} = \tau_{act} - (\tau_{cal} - \tau_{fpga} - \tau_{Tx} - \tau_{Rx}) \qquad (10)$$

where τ_{act} is the actual ToA based on geometry, τ_{cal} is the ToA from measurement calculations, τ_{fpga} is the delay in fpga from the transmit side as well as the receive side, τ_{Tx} and τ_{Rx} are the transmit and receive delays respectively. In Fig. 4, an experimental Cumulative Distribution Function (CDF) of the observed bias is plotted for all the sniffer antennas at measurement location ten. The five subplots in order are for sniffer locations one, two, three, four and five respectively. The blue and red curves are for the two vertically polarized antennas at each sniffer location.

These data all have a median delay bias of less than 5 ns, indicating a high degree of calibration of the system prior to deployment. However, tests in the lab consistently demonstrated subnanosecond synchronization and there is no reason to expect less than that here. The best explanation for the bias error is the presence of unresolvable multipath. If there exists a multipath component that is 16.27 ns away from the LOS path, then this path will not be resolvable with the bandwidth of our system and will lead to an erroneous estimation of the time of arrival. This is especially evident in the last subplot in Fig. 4. For this location there was less that 30cm (about 1 ns) difference in the path for the blue and red curves but the curves show a difference in bias of approximately 5 ns.

For the all links at point 10, the standard deviation is small but it is important to note that the median value of the two antennas for sniffer 5 is around four nanoseconds. The White Rabbit clock is not likely to be responsible for this errors rather it is most likely a result of unresolvable multipath; either scattering from the ground around the transmitter or from the building near the sniffer antennas.

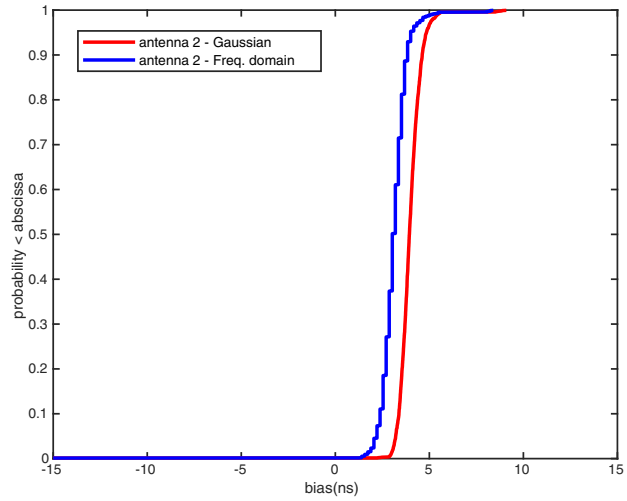

Fig. 5: Empirical CDF obtained by Gaussian interpolation and Frequency domain interpolation at the sniffer location five for one vertically polarized antenna for measurement location 10

Although we have analysed all the interpolation methods described in II-B the Gaussian method produces the lowest error and will confine our subsequent discussion to this

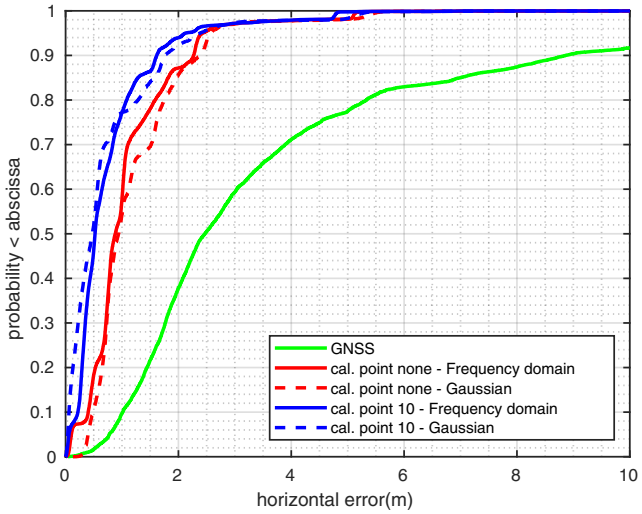

Fig. 6: Comparison of empirical CDF of horizontal localization error for WLLS with bias removal and for GNSS using Frequency domain and Gaussian interpolation

method. In Fig. 5, the blue curve is the 5th subplot of Fig. 4. The interpolation in this case was in the frequency domain. As a comparison, the red curve is the ToA bias for the same data when using the Gaussian interpolation method. There is remarkable agreement indicating that the high complexity of the frequency domain interpolation is unnecessary.

In the next section, the biases from the LoS location ten will be subtracted from the measured ToA in an attempt to remove any inherent timing biases and the localization will be calculated using the WLLS technique. While alternative bias corrections techniques have been discussed in [4] this simple bias correction and no bias correction at all will serve to illustrate the impact of the interpolation technique.

V. Localization Results

There are many choices for determining localization from time of arrival. In this paper, one of the most computationally simple choices, WLLS [2], [16] is used. We observed that there is a large discrepancy between the expected ToA and the estimated ToA in a known NLOS site. Such a large error in the ToA will create difficulties in convergence of WLLS solution. Therefore, an additional weighting was used to limit the impact of those sniffers that appeared to be in high multipath environments. The weighting was based on the number of peaks in the correlation that were above a threshold and inside the temporal region of interest. The results of the WLLS calculation are presented as empirical CDFs that are expressed as the rms error in the horizontal plane (xy-plane). The z-error was also computed but the horizontal result are sufficient to illustrate the advantages of the reduced complexity interpolation. Measurement point ten was used as the calibration point but the case of no calibration is also presented. The results for the horizontal localization are shown in Fig. 6 which shows the an experimental Cumulative

TABLE I: Constrained horizontal errors for various interpolation methods used

Interpolation method	**Bias Correction**	**xy error(m)**	
		median	$90^{th}\%$
	GNSS	2.471	8.88
Time domain	None	0.9434	2.272
	Meas point 10	0.9795	1.749
Frequency domain	None	0.88	2.28
	Meas point 10	0.52	1.63
Parabolic	None	1.136	2.344
	Meas point 10	1.137	2.149
Gaussian	None	0.9385	2.391
	Meas point 10	0.4728	1.735
Cosine	None	1.1	2.35
	Meas point 10	1.018	2.075
Two-point	None	1.455	2.779
	Meas point 10	1.531	2.265

Distribution Function (CDF) for the horizontal error with the frequency domain interpolation and Gaussian interpolation methods used respectively. The solid blue curve is for the solution in which the biases from measurement point ten were removed from all ToA and the frequency domain interpolation was employed. The red curve is for no bias removal and with frequency domain interpolation. Similarly, the dashed blue and red curves uses the Gaussian interpolation method. Finally, the green curve is for the GNSS data, taken with a u-blox M8T GNSS receiver used as a comparison. In all cases of bias removal and in both cases of interpolation, the sniffer system had significantly better localization performance than the GNSS system. Furthermore, there was virtually no degradation in the localization performance using the Gaussian interpolation method.

The results for horizontal errors are summarized in Table I in which the median and 90^{th} percentile errors are compared for all the curves shown in Fig. 6.

TABLE II: Comparison of processing times for various interpolation methods used for ToA computation

Interpolation method	Time domain	Frequency domain	Parabola	Gaussian	Cosine	Two-point
Processing time (s)	0.476	0.426	0.02	0.014	0.014	0.128

The computational time to perform the ToA computation is recorded in Table II. It should be noted that, these interpolation methods used (except for Frequency domain) have not been optimized and represent a naive implementation that should be able to achievable without difficulty. The program was run on MATLAB 2018b on a single core of Intel core i7-8050u CPU at a clock speed of 1.9 GHz with 16 GB RAM. Table II shows the mean CPU time required to estimate one delay value for each method. The Gaussian and Cosine interpolation method is the fastest, with the Gaussian providing a better localization accuracy among other three-point and two-point interpolation methods, hence provides a promising solution to track a multitude of object and vehicle at a rate of many times per second.

VI. Conclusions

A measurement driven evaluation of synchronized uplink ToA localization system has been discussed. While the localization challenges such as a) accurate location and b) accurate synchronization of the sniffers are solved in our previous work by employing White Rabbit protocol and by extensive conventional surveying, we mainly focused on challenge of c) accurate determination of ToA in this paper. To accomplish the ToA estimation, we proposed computationally efficient interpolation method in contrast to traditional processing intensive frequency domain interpolation. The location results demonstrated sub-meter accuracy with a 30 fold improvement in the computational efficiency at no cost of localization accuracy which promises that with our computationally efficient ToA algorithm, more users can be tracked more frequently and hence this would enable the localization network to better coordinate many simultaneous users.

References

[1] E. Günes and G. Ibarra, "Intranav—low-cost indoor localization system & iot platform," *Microsoft Indoor Competition*, vol. 2016, 2016.

[2] C. Gentile *et al.*, "Ranging and localization in harsh multipath environments," in *Geolocation Techniques*. Springer, 2013, pp. 17–57.

[3] F. Perez-Cruz, C.-K. Lin, and H. Huang, "Blade: A universal, blind learning algorithm for toa localization in nlos channels," in *Proceedings of IEEE Globecom Workshops*. IEEE, 2016, pp. 1–7.

[4] M. MacDonald, J. Pastalan, and D. Samardzija, "Experimental study of time of arrival localization using a highly synchronous wireless network," (under review).

[5] E. Kaplan and C. Hegarty, *Understanding GPS: principles and applications*. Artech house, 2005.

[6] G. Jacovitti and G. Scarano, "Discrete time techniques for time delay estimation," *IEEE Trans. on signal processing*, vol. 41, no. 2, pp. 525–533, 1993.

[7] L. Zhang and X. Wu, "On the application of cross correlation function to subsample discrete time delay estimation," *Digital Signal Processing*, vol. 16, no. 6, pp. 682–694, 2006.

[8] J. De *et al.*, "Experimental evaluation of the correlation interpolation technique to measure regional tissue velocity," *Ultrasonic imaging*, vol. 13, no. 2, pp. 145–161, 1991.

[9] J. De, PGM, T. Arts, A. Hoeks, and R. Reneman, "Determination of tissue motion velocity by correlation interpolation of pulsed ultrasonic echo signals," *Ultrasonic Imaging*, vol. 12, no. 2, pp. 84–98, 1990.

[10] E. Z. Psarakis and G. D. Evangelidis, "An enhanced correlation-based method for stereo correspondence with subpixel accuracy," in *Proceedings of Tenth IEEE ICCV'05*, vol. 1. IEEE, 2005, pp. 907–912.

[11] "Nikon Nivo 3M+ total station 3 second accuracy, 300m reflectorless range., http://www.dutasurveying.com/nikon-nivo-3m-3-second-reflectorless-total-station-hna303df.html, Accessed: 03-02-2020."

[12] P. Moreira *et al.*, "White rabbit: Sub-nanosecond timing distribution over ethernet," in *Proceedings of ISPCS*. IEEE, 2009, pp. 1–5.

[13] M. Lipiński, T. Włostowski, J. Serrano, and P. Alvarez, "White rabbit: A ptp application for robust sub-nanosecond synchronization," in *Proceedings of ISPCS*. IEEE, 2011, pp. 25–30.

[14] K. Sun, "Signal acquisition and tracking loop design for gnss receivers," *Geodetic Sciences: Observations, Modeling and Applications*, p. 1, 2013.

[15] J. D. Kraus, M. Tiuri, A. V. Räisänen, and T. D. Carr, *Radio astronomy*. Cygnus-Quasar Books Powell, Ohio, 1986, vol. 69.

[16] J. J. Caffery and G. L. Stuber, "Overview of radiolocation in cdma cellular systems," *IEEE Comms. Magazine*, vol. 36, no. 4, pp. 38–45, 1998.